J Wood Sci (2009) 55:409–416
DOI 10.1007/s10086-009-1049-x

ORIGINAL ARTICLE

Noritsugu Terashima · Kohei Kitano · Miho Kojima
Masato Yoshida · Hiroyuki Yamamoto · Ulla Westermark

Nanostructural assembly of cellulose, hemicellulose, and lignin in the middle layer of secondary wall of ginkgo tracheid

Received: May 28, 2009 / Accepted: June 24, 2009 / Published online: September 16, 2009

Abstract Physical, chemical, and biological properties of wood depend largely on the properties of cellulose, noncellulosic polysaccharides, and lignin, and their assembly mode in the cell wall. Information on the assembly mode in the main part of the ginkgo tracheid wall (middle layer of secondary wall, S2) was drawn from the combined results obtained by physical and chemical analyses of the mechanically isolated S2 and by observation under scanning electron microscopy. A schematic model was tentatively proposed as a basic assembly mode of cell wall polymers in the softwood tracheid as follows: a bundle of cellulose microfibrils (CMFs) consisting of about 430 cellulose chains is surrounded by bead-like tubular hemicellulose–lignin modules (HLM), which keep the CMF bundles equidistant from each other. The length of one tubular module along the CMF bundle is about 16 ± 2 nm, and the thickness at its side is about 3–4 nm. In S2, hemicelluloses are distributed in a longitudinal direction along the CMF bundle and in tangential and radial directions perpendicular to the CMF bundle so that they are aligned in the lamellae of tangential and radial directions with regard to the cell wall. One HLM contains about 7000 C_6-C_3 units of lignin, and 4000 hexose and 2000 pentose units of hemicellulose.

Key words Cellulose microfibril · *Ginkgo biloba* · Hemicellulose · Lignin · Nanostructure

N. Terashima[1] (✉) · U. Westermark[2]
STFI (Swedish Pulp and Paper Research Institute), Stockholm, Sweden

K. Kitano · M. Kojima · M. Yoshida · H. Yamamoto
Laboratory of Biomaterial Physics, Graduate School of Bioagricultural Sciences, Nagoya University, Nagoya 464-8601, Japan

Present address:
[1]2-610 Uedayama, Tenpaku, Nagoya 468-0001, Japan
Tel. +81-52-782-0981; Fax +81-52-782-0981
e-mail: norteras@quartz.ocn.ne.jp
[2]Hörnåkers vägen 45, 18365 Täby, Sweden

Part of this article was presented at the 59th Annual Meeting of the Japan Wood Research Society, Matsumoto, Japan, March 2009

Introduction

In the growing stems of trees, xylem cell walls are formed by successive deposition of pectic substances, cellulose, hemicellulose, and lignin.[1] Physical, chemical, and biological properties of wood depend largely on the first-order and higher-order structures of each cell wall component, and three-dimensional (3D) assembly mode of those polymers in the cell wall. Information on this assembly mode in nanoscale (nanostructure) is essential for a deeper understanding of the unique properties of wood and for new developments in forestry and the forest industry, which are intimately related to the mitigation of global warming.

Ginkgo (*Ginkgo biloba*), a so-called living fossil tree, retains primitive features of the tree cell wall that appeared in the early stages of tree evolution. Ginkgo tracheid walls are quite morphologically similar to those of representative conifers, and ginkgo does not form typical compression wood.[2] Ginkgo is one of the most suitable tree species for applying radioactive and stable isotope tracer techniques that provide information on the chemical structure, higher-order structure, and assembly process of the cell wall polymers during the formation of tracheid wall by nondestructive methods.[3,4] Normal wood of a representative conifer such as Japanese black pine (*Pinus thunbergii*) or sugi (*Cryptomeria japonica)* has a similar nanostructural assembly of polymers to that of ginkgo.[5]

During biogenesis of the cell wall, a small unit of cellulose microfibril (CMF) is synthesized by a rosette in the presence of noncellulosic polysaccharides,[1] and different numbers of CMFs form different sizes of bundles depending on the noncellulosic polysaccharides that associate with the nascent CMF.[1,6,7] This size of CMF bundle differs greatly depending on the cell wall layers in the ginkgo tracheid.[6,7] It has been observed that during the formation of the major part of ginkgo tracheid wall (middle layer of secondary wall: S2), CMF bundles coated with hemicellulose (possibly galactoglucomannan) are laid down slightly changing the orientation on the innermost surface of the tracheid followed by successive deposition of hemicellulose (possibly

arabino-4-*O*-methylglucuronoxylan) and lignin on the CMF bundle.[6,7] As a result, CMF bundles are embedded with lignin–carbohydrate complex (LCC) to form a composite of [CMF bundle + LCC]. The cross section examined under high resolution by field-emission scanning electron microscopy (FE-SEM) shows the cut ends of CMF bundles restrained in a slightly twisted honeycomb-like distribution by the LCC at equal distance from one another. The LCC surrounds a CMF bundle in the form of a tubular bead-like assembly unit "module" at a regular interval of about 16 ± 2 nm along the CMF-bundle.[6,7]

Estimation of the sizes of the CMF bundle, the hemicellulose–lignin module (HLM), and the unit composite [CMF bundle + HLM] can provide valuable information on the assembly mode of the cell wall polymers from a quantitative viewpoint. However, it is difficult to estimate the width of a CMF bundle by observation under electron microscopy, because the CMF bundle is covered with associated hemicellulose at an early stage of its formation in the cell wall. Removal of lignin and hemicellulose causes immediate formation of very large aggregates of CMFs.[6,7] In addition, observation by electron microscopy requires specimen pretreatments such as coating, staining, or replication that may cause undesirable artifacts or uncertainties.

In the present work, the width of a CMF bundle in S2 of the ginkgo tracheid wall was estimated by a new approach in which the above problems were circumvented. This new approach is based on the fact that the smallest assembly unit of cell wall polymers in S2 can be regarded as a composite made of a short (16 nm long) polygonal prism of CMF bundles covered with a short (16 nm long) tube of HLM. If the volume and density of the unit composite [CMF bundle + HLM], weight percent, and density of the CMF bundle are known, the volume percent (proportional to size) of the CMF can be estimated. A similar approach can be applied for the estimation of spaces occupied by hemicelluloses and lignin as well as their assembly mode in HLM. Results are combined in a simplified speculative view of assembly of the major components in S2 of gingko tracheid.

Experimental

Preparation of S2-rich ginkgo fiber and its chemical analyses

Ginkgo wood fibers rich in S2 were collected by beating ginkgo wood chips in water using a British disintegrator or a grater and a mixer. This was followed by density separation of the heavy S2-rich fiber fraction (Fig. 1a) from the light fraction rich in compound middle lamella (CML) and outer secondary wall (S1) (Fig. 1b) that sediments slower than the former fraction in water. Complete removal of the latter fraction from S2 was difficult, and a small amount of the contaminant was deemed negligible in this experiment. Holocellulose was prepared from the S2-rich fiber by the Wise method,[8] and α-cellulose content was determined by treatment of the holocellulose with 17.5 % aqueous sodium hydroxide to remove hemicelluloses according to the methods described by Browning.[8] Lignin content was determined from the ultraviolet (UV) absorbance of a solution of S2-rich fiber dissolved in a mixture of acetyl bromide and acetic acid.[9] Ginkgo milled wood lignin (MWL) was prepared by conventional methods and its absorptivity (20.09 $lg^{-1}cm^{-1}$ at 280 nm) was used for the determination.

Determination of density

For determination of the density, finely cut samples (about 60 mesh) were suspended in a mixture of carbon tetrachloride and dioxane by applying vibration. The density of the mixture kept in suspension after applying centrifugal force (8000 *g*, 5 min) was regarded as the density of the sample.

Examination by FE-SEM

Small blocks that included differentiating xylem were cut from the normal wood part of a 4-year-old growing stem of ginkgo in June, and fixed with 3% glutaraldehyde in 0.1 M phosphate buffer for 1 day followed by washing with the same buffer and stored in a refrigerator. At first, a tangential section (about 0.5–1 mm thick, 5 mm wide, 20 mm long) was prepared from the xylem part, and the microfibril angle (MFA) of the section was determined by X-ray diffraction.[10] A cross section and a radial section (about 300–500 μm thick × 3 mm × 3 mm) inclined at the predetermined MFA and [90° + MFA] respectively were prepared from the ginkgo xylem using a sliding microtome equipped with a freezing sample stage. Selective delignification was carried out by heating the section with sodium chlorite (15 mg/section) in acetate buffer (pH 3.5, 2 mM, 1 ml) at 75°C for 6 hours. The treatment was repeated four times, and complete removal of lignin was confirmed by examination of a epoxy resin-embedded section under an UV microscope as described in a previous report.[7] A section was stained with 1% potassium permanganate in 0.1% sodium citrate aqueous solution for 3 min (Fig. 1h). The sections were dehydrated in a series of graded ethanol–water solutions followed by freeze drying using *t*-butanol, and coated with approximately 2 nm total thickness of osmium and platinum/palladium using an osmium coater (HPC hollow cathode CVD osmium coater) and an ion-sputter (Hitachi E-1030). These sections were examined using a FE-SEM (Hitachi S-4500) at an accelerating voltage of 1.5 kV and working distance of 3–5 mm. It was confirmed by changing the scanning direction that the images of fine materials shown in Fig. 1f, i, and j are not artifacts caused by scanning noise.

Results and discussion

Experimentally determined and theoretically deduced values are summarized with short explanations in Tables 1 and 2. At the diagonally cut area of S2 (Fig. 1c), cut ends

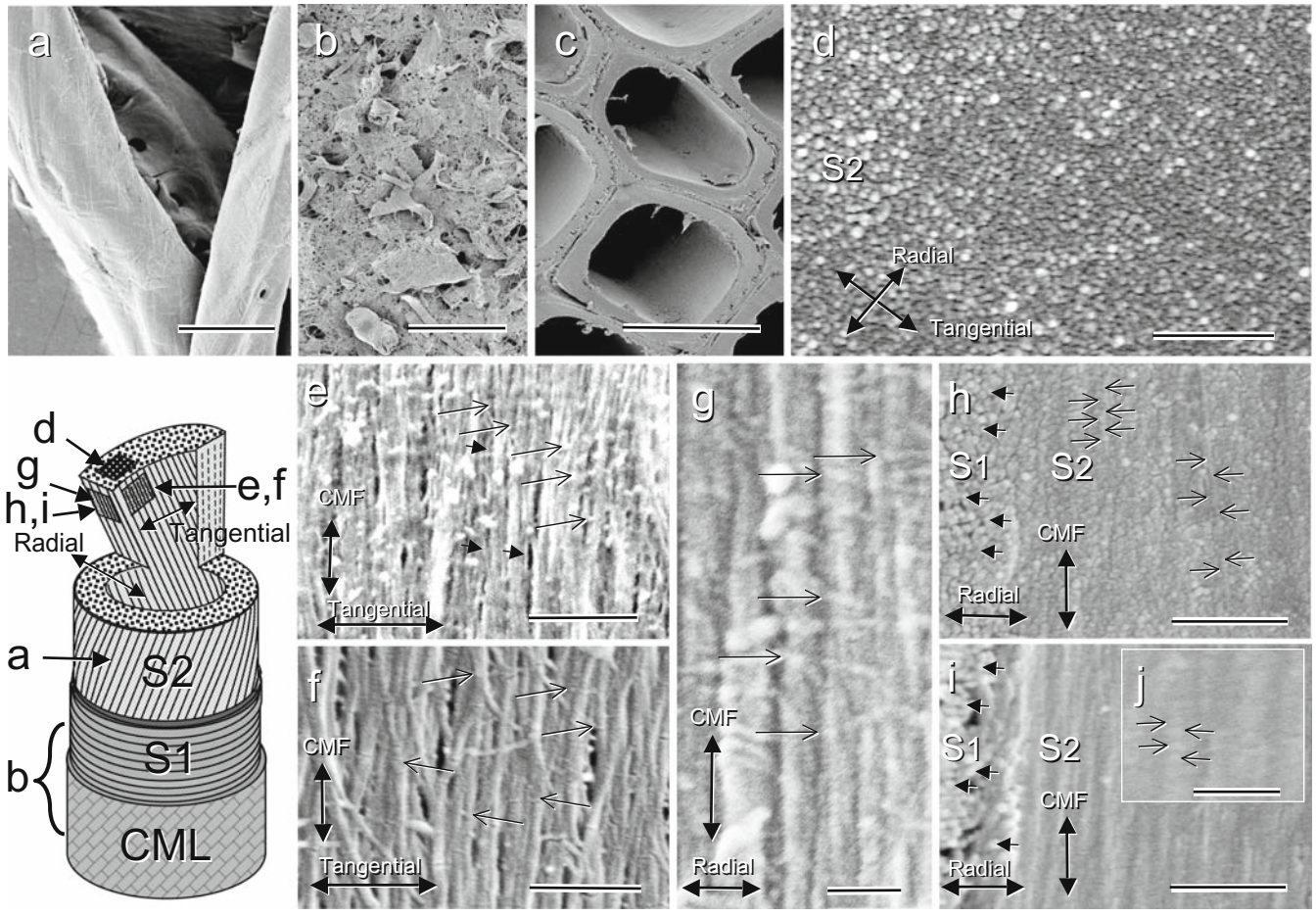

Fig. 1a–j. Field-emission scanning electron microscopy (FE-SEM) micrographs of the illustrated areas (*bottom left*) of ginkgo tracheid. **a** S2-rich ginkgo fiber. **b** Low-density fragments rich in S1 and compound middle lamella (CML). **c** Cross section cut at an inclination angle of 30° that corresponds to microfibril angle (MFA). **d** Part of cross-cut S2 perpendicular to cellulose microfibril (CMF) bundle. **e** Innermost surface of differentiating ginkgo tracheid at S2 formation stage. *Small arrows* indicate fibrillar structures forming nodes at the cross-linking points on the CMF bundles. *Arrowheads* indicate some thin branch CMFs liberated from CMF bundle and join another bundle. **f** Innermost surface of differentiating ginkgo tracheid at S2 formation stage, after delignification treatment. Fine fibrillar structures of hemicellulose are cross-linking the CMF bundles (*small arrows*). **g** Radial plane parallel to CMF bundle at an early stage of S2 formation. *Small arrows* indicate fibrillar structures cross-linking the CMF bundles with nodes on them. **h** Radial plane parallel to CMF bundle at a later stage of S2 formation. *Arrowheads* in S1 indicate cross-cut ends of CMF bundles, *small arrows* in S2 indicate bead-like structures (hemicellulose–lignin modules, HLMs) surrounding the CMF bundle. **i** Radial plane parallel to CMF bundle at later stage of S2 formation, after mild removal of lignin. Most of the bead-like structures in S2 disappeared with lignin removal, while cross-cut ends of CMF bundles in S1 (*arrowheads*) were retained. **j** Enlarged image of a part of **i**. Fine structure of hemicellulose with nodes (*small arrows*) are observed, and CMF bundles are hidden behind them. *Bars* **a–c**, 20 μm; **d–f**, **h**, **i**, 300 nm; **g**, **j**, 100 nm

Table 1. Dimension, density, and volume of unit composite [CMF bundle + HLM], CMF bundle, and HLM in S2

Determined or estimated item	Value	Procedure or explanation
(1) Length of tubular HLM and covered CMF bundle	16 ± 2 nm	From previous works[5,6], see text
(2) Cross-sectional area of [CMF bundle + HLM]	309 ± 18 nm^2	From FE-SEM micrograph (Fig. 1d), see text
(3) Width of [CMF bundle + HLM]	17.6 ± 0.5 nm	Cross section was regarded as square, see text
(4) Volume of one [CMF bundle + HLM]	4944 ± 288 nm^3	(1) × (2)
(5) Density of [CMF bundle + HLM]	1.45 g/cm^3	Density of S2-rich fiber suspended in CCl_4–dioxane
(6) CMF% in [CMF bundle + HLM] (= α-cellulose content)	46.1%	α-Cellulose content was regarded as CMF content
(7) Density of CMF bundle	1.52 g/cm^3	Density of α-cellulose suspended in CCl_4–dioxane
(8) Volume% of CMF bundle in S2	44.0%	(6) × (5) / (7)
(9) Cross-sectional area of one CMF bundle	136 ± 10 nm^2	(2) × (8)
(10) Width of CMF bundle	11.7 ± 0.4 nm	Cross section of CMF bundle was regarded as square
(11) Cross-sectional area of one cellulose chain	0.317 nm^2	From the lattice parameters of cellulose crystal Iβ
(12) Number of cellulose chains in a single CMF bundle	429 ± 32	(9) / (11)
(13) Number of the smallest unit CMFs in a CMF bundle	12	It was assumed that one rosette produces 36 cellulose chains
(14) Cross-sectional area of HLM	173 ± 9 nm^2	(2) − (9)
(15) Thickness of tubular HLM at its side	3 ± 0.5 nm	[(3) − (10)] / 2

CMF, Cellulose microfibril; HLM, hemicellulose–lignin module; FE-SEM, field-emission scanning electron microscopy

Table 2. Quantitative estimation and deduction about hemicelluloses and lignin in HLM

Determined or deduced item	Value	Procedure or explanation
(16) Volume of HLM	2768 ± 150 nm^3	(14) × (1) (Average length of HLM along CMF: 16 nm)
(17) Weight of HLM	3864 ± 210 ng	(4) × (5) × [100% − (6)]
(18) Content of lignin in [CMF bundle + HLM]	32.10%	Determined by UV absorbance of S2-rich fiber, see text
(19) Content of hemicellulose in [CMF bundle + HLM]	21.80%	100% − (6) − (18)
(20) Weight of lignin in HLM	2301 ± 124 ng	(17) × (18) / (18 + 19)
(21) Weight of a C_6-C_3 unit in *β-O*-4 polylignol	0.326 ng	$C_{10}H_{12}O_4$: 196.2 g / 6.022 × 10^{23}
(22) Number of lignin C_6-C_3 units in HLM	7058 ± 380	(20) / (21)
(23) Weight of hemicellulose in HLM	1563 ± 85 ng	(17) × (19) / (18 + 19)
(24) Ratio of mannan to xylan (≈ ratio of hexosan to pentosan)	5:2	Chemical analysis by Timell,[20–22] see text
(25) Weight of galactoglucomannan in HLM	1116 ± 61 ng	(23) × 5 / 7
(26) Weight of arabino-4-*O*-methylglucuronoxylan in HLM	447 ± 25 ng	(23) × 2 / 7
(27) Weight of hexose unit $C_6H_{10}O_5$ in galactoglucomannan	0.269 ng	$C_6H_{10}O_5$: 162.1 g / 6.022 × 10^{23}
(28) Weight of penose unit $C_5H_8O_4$ in arabinoglucuronoxylan	0.219 ng	$C_5H_8O_4$: 132.1 g / 6.022 × 10^{23}
(29) Number of hexose units in HLM	4149 ± 227	(25) / (27), hexose assumed to be in galactoglucomannan
(30) Number of mannan chain fragments included in HLM	134	One mannan chain, 16 nm long, includes 31 pyranose units
(31) Number of pentose units across the HLM	2041 ± 114	(26) / (28), pentose assumed to be in arabinoglucuronoxylan
(32) Number of xylan chain fragments across the HLM	60	One xylan chain, 17.6 nm long, includes 34 pyranose units
(33) Density of lignin in HLM	1.36 g/cm^3	Density of periodate lignin, see text
(34) Volume of lignin in HLM	1692 ± 92 nm^3	(20) / (33)
(35) Volume of hemicellulose in HLM	1076 ± 242 nm^3	(16) − (34)
(36) Volume ratio of lignin to hemicellulose in HLM	3:2	(34):(35)

of CMF bundles in the plane perpendicular to their orientation are observed in a honeycomb-like distribution (Fig. 1d). The cross-sectional area of one [CMF bundle + HLM], determined by counting the number of cut ends of CMF bundles in a given area, was 309 ± 18 nm^2 (Table 1).

Figure 1e shows the innermost surface of the tracheid wall at S2 formation stage, where fibrillar materials are depositing across the CMF bundles with nodes at crossing points (small arrows) in a tangential direction to the cell wall. Figure 1f shows the innermost surface of the cell wall after mild removal of lignin. Fine fibrillar materials (small arrows) crosslinking between CMF bundles remained after delignification. Those fibrils thinner than the CMF bundle in Fig. 1f are regarded as hemicellulose, and the thick fibrillar materials with nodes observed before delignification (Fig. 1e) may be a kind of complex composed of hemicellulose and lignin anchor such as ferulic acid or oligolignols. Hafrén et al.[11] observed similar crosslinks between CMFs by thin fibrils in delignified pine S2 by a combination of a rapid-freeze deep-etching technique and transmission electron microscopy.

Figure 1g shows the radial plane parallel to a CMF bundle at an early stage of S2 formation. Fibrillar materials (small arrows) crosslink the CMF bundles with nodes at crossing points. Those nodes grow to bead-like modules (HLMs) surrounding the CMF bundle with average intervals of 16 nm in the mature S2 (Fig. 1h, small arrows). Those bead-like HLMs in S2 disappeared after mild selective removal of lignin (Fig. 1i), and CMF bundles in S2 are hidden by the remaining fine hemicellulose with nodes at intervals similar to that of HLM (Fig. 1j, small arrows).

Thus, the CMF bundles are crosslinked by fibrillar material in tangential and radial directions perpendicular to the CMF bundle, and a kind of lamella structure is formed in these two directions (Fig. 1d). Therefore, it is reasonable to regard the cross section of [CMF bundle + HLM] as almost square, with an estimated width of 17.6 ± 0.5 nm (Table 1, Fig. 2). Fahlén and Salmén[12] examined S2 of spruce tracheid by atomic force microscopy, and assumed that the cross section of the fiber corresponding to the unit composite [CMF bundle + HLM] was square with a side length around 18 nm, which is close to the estimated width of the composite in ginkgo S2.

On the assumption that *α*-cellulose content can be regarded as the content of CMF, the cross-sectional area of the CMF bundle was estimated to be about 136 nm^2 as shown in Table 1. Based on the lattice parameters of cellulose crystal I*β*,[13] which is dominant in S2,[14] cross-sectional area occupied by one cellulose chain is calculated to be 0.317 nm^2 (Table 1). Assuming that the CMF bundle does not include hemicellulose or lignin inside the bundle, the estimated number of cellulose chains included in a single CMF bundle will be about 430 (Table 1). If 1 rosette synthesizes the smallest unit CMF consisting of 36 cellulose chains,[15] a single CMF bundle in S2 corresponds to a bundle of the unit CMFs produced by 12 rosettes. The true shape of the cross section of a bundle of 12 CMFs in ginkgo S2 is not known. It may be almost square as observed in the cellulose of *Valonia macrophysa*,[16] or parallelogram and hexagonal as observed in the cellulose of *Halocynthia papillosa*.[17] The 3D organization of CMFs in delignified radiata pine S2 was investigated by a new approach employing dual-axis electron tomography, and no regular cross section of a "CMF cluster" was reported.[18] To draw further deductions about the shape and thickness of tubular HLM in ginkgo S2, we tentatively presumed that the cross section of the CMF bundle is almost square with its side width about 12 nm (Table 1).

It is noted that the theoretical density of the cellulose crystal I*β* is 1.63, while the density of ginkgo *α*-cellulose was

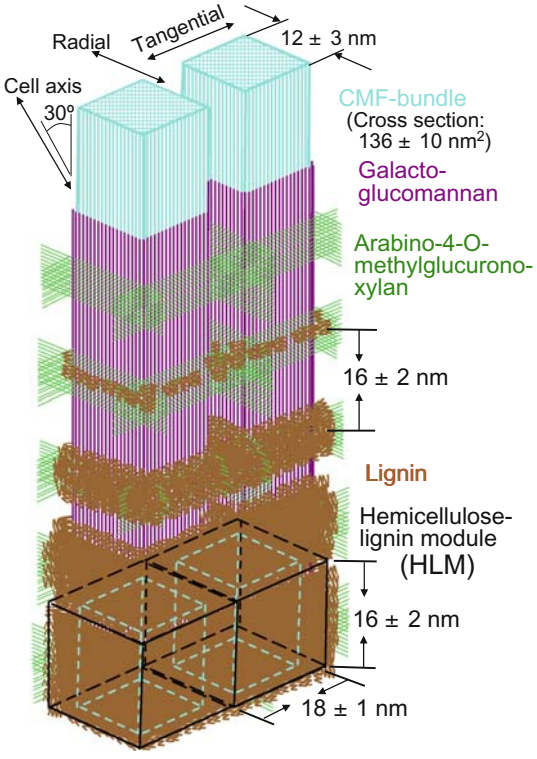

Fig. 2. Simplified speculative view of the assembly process (from top to bottom) of CMF bundle, hemicelluloses, and lignin with their approximate estimated sizes in S2

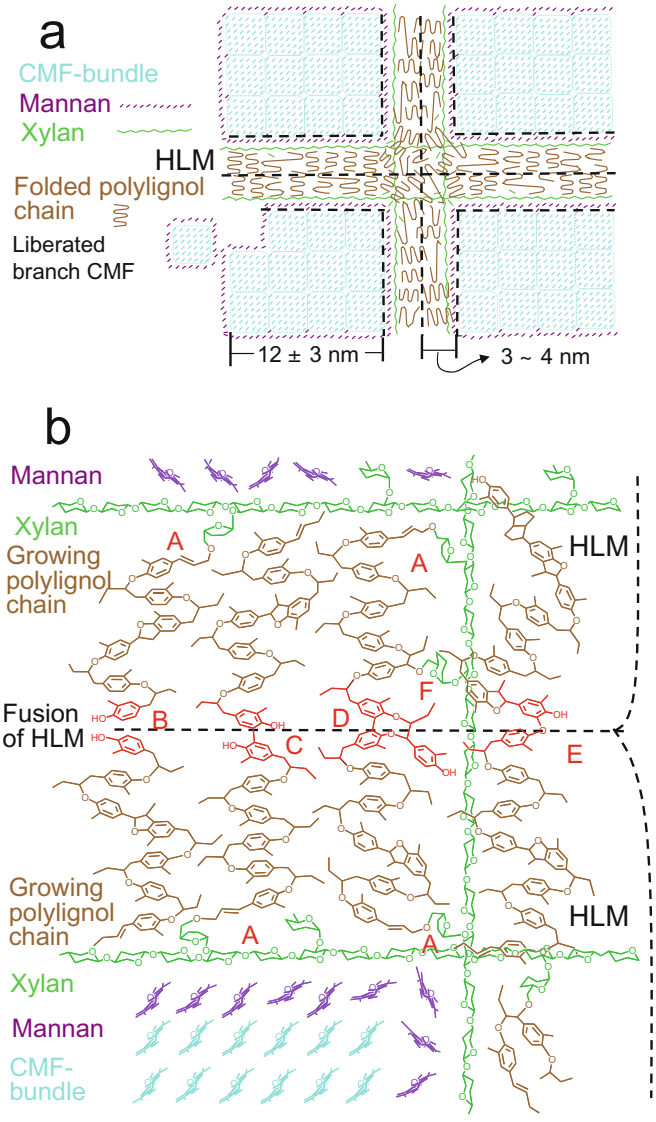

Fig. 3. **a** Simplified hypothetical cross-sectional view of the assembly mode of cellulose, lignin, and hemicelluloses in S2. **b** Possible mechanism of fusion of growing HLMs at their contact boundaries by formation of 5-5′, and 4-*O*-5′ linkages between growing polylignol chains. It was assumed that the lignin aromatic rings are statistically parallel to the cell wall surface (perpendicular to the page)

1.52, which is the same as the determined density of microcrystalline cellulose (Merck) and the G-layer isolated from tension wood of *Quercus acutissima*. This value suggests that 7% excess volume of α-cellulose compared with that of cellulose crystal Iβ may be occupied by low-density disordered cellulose chains and low-density crystal Iα at the outer part of the CMF[19] in addition to disordered aggregation regions between the individual CMFs in the bundle. It is not clear whether hemicellulose is involved inside the CMF bundle in ginkgo, but thin fibrils sometimes liberated from larger bundles join another bundle (Fig. 1e, arrowheads), and these fine fibrils associated with hemicelluloses (probably with glucomannan, as shown in Fig. 3a) may be partly included in the α-cellulose prepared in this experiment.

From the estimated cross-sectional area of [CMF bundle + HLM] and CMF bundle, the volume and weight of one tubular HLM can be deduced (Table 2). The weight of lignin and hemicellulose in the HLM was calculated as 2301 ng and 1563 ng, respectively, from the experimentally determined content of lignin and cellulose. From the theoretical weight of a C_6-C_3 monolignol unit in β-*O*-4 linked polylignol, it can be deduced that one HLM contains about 7000 C_6-C_3 lignin monomer units (Table 2).

Based on the results of chemical analyses of the major hemicelluloses in ginkgo wood,[20–22] the approximate ratio of galactoglucomannan to arabino-4-*O*-methylglucuronoxylan is about 5:2, and the weight of the hemicelluloses in HLM can be estimated. It is deduced from the theoretical weights of single hexose and pentose units that one HLM contains about 4000 and 2000 of these monosaccharide units, respectively, as the main monomeric units of galactoglucomannan and arabino-4-*O*-methylglucuronoxylan, respectively (Table 2).

Assembly of hemicellulose and CMF

It has been shown by immunological labeling that the matrix that deposits on the CMF during the S2 formation stage of a sugi tracheid contains glucomannan and xylan.[23,24] However, it is not yet known how galactoglucomannan and arabino-4-*O*-methylglucuronoxylan participate in the deposition process of CMF bundles and crosslinking of

the bundles in differentiating S2. Model experiments on the association of hemicellulose and CMF have been carried out by formation of bacterial cellulose in the presence of acetyl glucomannan or glucuronoxylan as observed by immunogold labeling.[25,26] Glucomannan may play a role mainly in controlling the aggregation of CMF by associating with the nascent CMF, while glucuronoxylan associates locally with some intervals.[25,26] In delignified fiber secondary wall of beech, globular materials have been observed on CMFs, and the globular material was removed by treatment with xylanase.[27] Those observations suggest that arabino-4-*O*-methylglucuronoxylan may play an important role in periodical formation of tubular bead-like HLM on the CMF bundle.[6,7]

Assuming that the main chains of galactoglucomannan and arabino-4-*O*-methylglucuronoxylan penetrate HLM in their most extended linear state, 31 and 34 pyranose rings of about 0.52 nm long may exist in the HLM in a direction parallel to CMF (16 nm) or a perpendicular direction to CMF (17.6 nm), respectively. Then the number of galactoglucomannan chain fragments included in HLM will be about 134 (Table 2), which is 1.6 times larger than the 84 cellulose chains at the outermost part of the CMF bundle. Galactoglucomannan may associate with cellulose mostly at the surface of a CMF bundle, partly at the surface of thin CMF included in the bundle[25] and partly on the branch CMFs that interconnect two bundles as seen in Fig. 1e (arrowheads) and illustrated in Fig. 3a. On the one hand, the number of arabino-4-*O*-methylglucuronoxylan chain fragments penetrating a HLM will be about 60 (Table 2), and these chains may surround four sides of a CMF bundle as shown in the simplified speculative view, Figs. 2 and 3.

The length of the main xylan chain estimated from the structure of arabino-4-*O*-methylglucuronoxylan in ginkgo (number-average polymerization degree, DP = 185, xylose:arabinose:acid = 180:2:3)[21] is around 94 nm, which is long enough to penetrate through five units of [CMF bundle + HLM] in its extended linear state. On the other hand, the estimated main chain length of galactoglucomannan (DP = 96, mannose:glucose:galactose = 72:20: 4)[22] is around 48 nm, and that may be too short to crosslink more than two CMF bundles. It has been suggested that ferulate on arabinoxylan plays a role as initiation or nucleation sites for lignification in grasses.[28,29] In ginkgo, a bundle of about 60 arabino-4-*O*-methylglucuronoxylan chains crosslinking between CMF bundles in the radial and tangential directions at about 16-nm intervals may play a similar role in lignification of ginkgo S2 as shown in Figs. 2 and 3b.

Assembly of hemicellulose and lignin in HLM, and possible fusion of HLMs at their surface

When cross sections of the composite [CMF bundle + HLM] and CMF bundles are assumed to be square, the thickness of the tubular HLM will be about 3 nm at its side (Table 1, Fig. 3a). Information on the densities of lignin will provide further quantitative deduction on the assembly mode of lignin in HLM. However, it is difficult to directly determine the real density of protolignin in the cell wall because the protolignin exists as a compact lignin–polysaccharide complex. The density of isolated lignin such as dioxane lignin (1.278 g/cm^3)[30] is much lower than that of periodate lignin (1.350 g/cm^3),[30] which retains its original macromolecular structure. Employing the density of sugi periodate lignin prepared by an improved procedure,[31] the ratio of the space occupied by lignin and hemicelluloses can be estimated to be about 3:2 (Table 2). The most abundant interunit linkage in ginkgo protolignin is β-*O*-4,[4] and a study employing a β-*O*-4-linked oligolignol structural model indicates that the linear chain is folded so that the aromatic ring planes are nearly parallel when this compound occurs in the most compact state.[1] The estimated distance between two aromatic ring planes is about 0.3–0.4 nm.[1] Raman microprobe spectra from the secondary wall of spruce showed that the protolignin aromatic rings are parallel to the cell wall surface.[32,33] This suggests that lignin occupies about 60% of the side space of HLM. Five to seven lignol units probably folded at 0.3–0.4 nm may occupy about a 1.8- to 2.4-nm-thick space of the side (about 3 nm) of HLM as illustrated in the simplified speculative view of Fig. 3a.

If an initiation point for polymerization of lignols is a kind of phenolic acid such as ferulic acid bound on xylan (Fig. 3b, A) as in grass lignin,[28,29] the folded polylignol chain will grow in a radial direction keeping the parallel orientation of aromatic rings toward the interspace between two CMF bundles (Fig. 3b, B). When two growing ends of polylignol chains are forced into contact, 5-5′ or 4-*O*-5′ linkages will be formed (Fig 3b, C and E). It is noted that 5-5′-linked or 4-*O*-5′-linked dimers of coniferyl alcohol are not formed from the monomer by in vitro dehydrogenative polymerization.[34] These types of biphenyl linkages will be formed only when the two growing ends are forced (partly by limited free rotation by lignin–hemicellulose bonds such as shown in Fig. 3b, F) into close proximity and supply or access of monomeric side chain radical is limited. If two growing chains meet in the same direction, 5-5′ bonding can be followed by further addition of a monolignol to form a dibenzodioxocin structure (Fig 3b, D). By two-dimensional nuclear magnetic resonance spectroscopic analysis of Japanese red pine MWL, Akiyama and Ralph[35] showed that further addition of a monolignol after the fusion of two growing chains is limited to only one, so that the phenolic hydroxyl group of dibenzodioxocin is free. Their finding seems to be reasonable from the consideration that when dibenzodioxocin is formed by fusion of two growing HLM at the final stage of lignification, available space after the fusion will not be sufficient for further chain growth (Fig. 3b, D). This speculative view of the lignin network formation by fusion of HLM lignin by 5-5′ and 5-*O*-4′ linkages and by lignin–polysaccharide bonds (Fig. 3b, F) is supported by the observation that selective removal of cellulose and hemicellulose by periodate oxidation followed by hydrolysis does not produce powdery lignin, and the periodate lignin retains the original morphological features of the cell wall.[31] Formation of condensed structure-rich lignin in an early stage of cell wall differentiation seems to be reasonable from the fact that the lignin in the first lignifying cell

corner and CML regions are globular lignin-rich modules and the fusion occurs at the whole surface of the randomly piled modules.[31] Immunolocalization of dibenzodioxocin substructures in the cell wall of Norway spruce[36,37] support the above speculative view.[31]

It should be noted that the frequency of the bond formation at the boundary of HLM is lower than that inside HLM. Therefore, the radial section prepared under freezing conditions retains a bead-like modular structure by tearing the weak-bonded boundary between frozen HLMs as shown in Fig. 1g,h. In an early stage of lignin deposition (Fig. 1g), incomplete fusion of immature HLM provides a well-separated image of the module, while at a later stage (Fig. 1h), densely packed modules can be observed by freeze-fracture using a sliding microtome equipped with a freezing sample stage.

Thus, the space between CMF bundles available for growth of polylignol is one of the important factors controlling lignin content and its macromolecular structure. The dimension of this space depends on the size, shape, and distance of CMF bundles, which are regulated by hemicelluloses during the formation of the cell wall.[6,7] In lignifying S1 of ginkgo, thin CMF bundles surrounded by larger globules of HLM have been observed.[6] Donaldson[38] reported an approximately linear relationship between lignin concentration and diameter of macrofibrils (proportional to [CMF bundle + HLM]) of different wood types.

Conclusions

Based on the information obtained by the new approach, a simplified speculative view of the assembly of cell wall polymers in ginkgo S2 was proposed as illustrated in Figs. 2 and 3. Starting from this hypothetical view, verification and modification of this tentative hypothesis in the future will provide a correct view of the true nanostructure of ginkgo tracheid wall.

The present work suggests that the cross section of the composite unit [CMF bundle + HLM] is almost square with a width of 18 ± 1 nm (Fig. 2), but the shape of the cross section of the CMF bundle is not known. Considering the possible parallelogramic or hexagonal cross section of a bundle of CMFs produced by 12 rosettes, we tentatively proposed its width as 12 ± 3 nm (Figs. 2 and 3a). Because the shape of the space available for lignin deposition in HLM depends on this cross section of the CMF bundle, its true shape will be one of the important research targets in the future.

Based on the model experiment, it was tentatively assumed that aggregation of unit CMFs to form a CMF bundle is controlled mainly by galactoglucomannan, and the distance between the CMF bundles is controlled mainly by arabino-4-*O*-methylglucuronoxylan. However, the exact role of these hemicelluloses in the formation of CMF bundles and HLM in a softwood tracheid and the mechanism of hemicellulose deposition, especially in the radial direction, are not yet fully understood. Answers to those questions will provide clues for understanding true cell wall nanostructure and for control of cell wall properties by genetic engineering in the future.

Properties of wood cell walls depend also on the assembly mode of cell wall polymers in S1 and compound middle lamella regions. More improved approaches are necessary for elucidation of the whole cell wall nanostructure.

Acknowledgments The authors are grateful to the research foundation Skogsindustrins Forskningsstiftelse for financing the stay of N.T. as a guest researcher at STFI, and to Mrs. Sally Ralph, USDA Forest Products Laboratory, Madison, USA, for her help in preparing the manuscript.

References

1. Terashima N, Fukushima K, He LF, Takabe K (1993) Comprehensive model of the lignified plant cell wall. In: Jung HG, Buxton DR, Hatfield RD, Ralph J (eds) Forage cell wall structure and digestibility. American Society of Agronomy, Madison, USA, pp 247–270
2. Timell TE (1986) Origin and evolution of compression wood. In: Compression wood in gymnosperms. Springer, Berlin Heidelberg New York, pp 597–621
3. Terashima N (2007) Non-destructive approaches to identify the ultrastructure of lignified ginkgo cell walls. Int J Plant Develop Biol 1:170–177
4. Terashima N, Akiyama T, Ralph S, Evtuguin D, Pascoal Neto C, Parkås J, Paulsson M, Westermark U, Ralph J (2009) 2D-NMR (HSQC) difference spectra between specifically ^{13}C-enriched and unenriched protolignin of *Ginkgo biloba* obtained in the solution state of whole cell wall material. Holzforschung 63:379–384
5. Terashima N, Yoshida M (2006) Observation of formation process of macromolecular lignin in the cell wall by electron microscope IV. Formation of hemicellulose-lignin module in black pine tracheid. Proceedings of the Annual Meeting of the Japan Wood Research Society Akita, Japan, PA005
6. Terashima N, Awano T, Takabe T, Yoshida M (2004) Formation of macromolecular lignin in ginkgo xylem cell walls as observed by field emission scanning electron microscopy. Comptes Rendus Biologies 327:903–910
7. Terashima N, Yoshida M (2005) Ultrastructural assembly of polysaccharides and lignin in lignifying plant cell walls. Proceedings of 13th International Symposium on Wood, Fiber, and Pulping Chemistry, Auckland, New Zealand, vol 2, pp 423–426
8. Browning BL (1967) Preparation of holocellulose by chlorite methods (Wise method) and determination of alpha-cellulose content. In: Methods of wood chemistry, vol 2. Interscience, New York, p 395, 418
9. Dence CW (1992) Determination of lignin in wood and pulp by the acetyl bromide method. In: Lin SY, Dence CW (eds) Methods in lignin chemistry, Springer, Berlin Heidelberg New York, pp 44–48
10. Yamamoto H, Okuyama T, Yoshida M (1993) Method of determining the mean microfibril angle of wood over a wide range by the improved Cave's method. Mokuzai Gakkaishi 39:375–381
11. Hafrén J, Fujino T, Itoh T (1999) Changes in cell wall architecture of differentiating tracheids of *Pinus thunbergiii* during lignification. Plant Cell Physiol 40:532–541
12. Fahlén J, Salmén L (2003) Cross-sectional structure of the secondary wall of wood fibers as affected by processing. J Mater Sci 38:119–126
13. Nishiyama Y, Langan P, Chanzy H (2002) Crystal structure and hydrogen-bonding system in cellulose Iβ from synchrotron X-ray and neutron fiber diffraction. J Am Chem Soc 124:9074–9082
14. Kataoka Y, Kondo T (1996) Changing cellulose crystalline structure in forming wood cell walls. Macromolecules 29:6356–6358
15. Herth W (1983) Arrays of plasma-membrane "rosettes" involved in cellulose microfibril formation of *Spyrogyra*. Planta 159: 347–356

16. Sugiyama J, Harada H, Fujiyoshi Y, Uyeda N (1985) Lattice images from ultrathin sections of cellulose microfibrils in the cell wall of *Valonia macrophysa* Kütz. Planta 166:161–168
17. Helbert W, Nishiyama Y, Okano T, Sugiyama J (1998) Molecular imaging of *Halocynthia papillosa* cellulose. J Struct Biol 124:42–50
18. Xu P, Donaldson LA, Gergely ZR, Staehelin A (2007) Dual axis electron tomography: a new approach for investigating the special organization of wood cellulose microfibrils. Wood Sci Technol 41:101–116
19. Baker AA, Helbert W, Sugiyama J, Miles MJ (2000) New insight into cellulose structure by atomic force microscope shows the Iα crystal phase at near-atomic resolution. Biophys J 79:1139–1145
20. Timell TE (1960) Studies on *Ginkgo biloba* L. 1. General characteristics and chemical composition. Sven Papperstidn 63:652–657
21. Mian J, Timell TE (1960) Studies on *Ginkgo biloba* L. 2. The constitution of an arabino-4-*O*-methyl-glucurono-xylan from the wood. Sven Papperstidn 63:769–774
22. Timell TE (1961) Isolation of galactoglucomannans from the wood of gymnosperms. TAPPI 44:88–96
23. Yoshida M, Hosoo Y, Okuyama T (2000) Periodicity as a factor in the generation of isotropic compressive growth stress between microfibrils in cell wall formation during a twenty-four hour period. Holzforschung 54:469–473
24. Hosoo Y, Imai T, Yoshida M (2006) Diurnal differences in the supply of glucomannanns and xylans in inner-most surface of cell walls at various developmental stages from cambium to mature xylem in *Cryptomeria japonica*. Protoplasma 229:11–19
25. Tokoh C, Takabe K, Sugiyama J, Fujita M (2002) Cellulose synthesized by *Acetobacter xylinum* in the presence of plant cell wall polysaccharides. Cellulose 9:65–74
26. Tokoh C, Takabe K, Sugiyama J, Fujita M (2002) CP/MAS ^{13}C NMR and electron diffraction study of bacterial cellulose structure affected by cell wall polysaccharides. Cellulose 9:351–360
27. Awano T, Takabe Y, Fujita M (2002) Xylan deposition on secondary wall of *Fagus crenata* fiber. Protoplasma 219:106–115
28. Ralph J, Grabber JH, Hatfield RD (1995) Lignin-ferulate cross-link in grasses: active incorporation of ferulate polysaccharide esters into ryegrass lignins. Carbohydr Res 275:167–178
29. Ralph J, Hatfield RD, Grabber JH, Jung H-JG, Quideau S, Helm RF (1998) Cell wall cross-linking in grasses by ferulates and diferulates. In: Lewis NG, Sarkanen S (eds) ACS Symposium Series 697, Lignin and lignan biosynthesis. American Chemical Society, Washington DC, pp 209–236
30. Ramiah MV, Goring DAI (1965) The thermal expansion of cellulose, hemicellulose, and lignin. J Polym Sci Part C 11:27–48
31. Terashima N, Yoshida M (2006) Ultrastructure of lignified plant cell wall observed by field-emission scanning electron microscopy. Observations on periodate lignin prepared from *Ginkgo biloba*. Cellulose Chem Technol 40:727–733
32. Atalla RH, Agarwal UP (1986) Raman microprobe evidence for lignin orientation in the cell wall of native woody tissue. Science 227:636–638
33. Agarwal UP, Atalla RH (1986) In-situ Raman microprobe studies of plant cell walls: macromolecular organization and compositional variability in the secondary wall of *Picea mariana* (Mill.) B.S.P. Planta 169:325–332
34. Terashima N, Attala RH (1995) Formation and structure of plant cell wall – factors controlling lignin structure during its formation. Proceedings of the 8th International Symposium on Wood and Pulping Chemistry, Helsinki. Finland, vol 1, pp 69–76
35. Akiyama T, Ralph J (2008) Characteristics in ^{1}H- and ^{13}C-NMR chemical shifts of non-phenolic dibenzodioxocin model compounds as branch-points in lignin. Proceedings of 53rd Lignin Symposium, Tokyo, pp 84–87
36. Kukkola E, Koutaniemi S, Pöllänen E, Gustafson M, Karuhnen P, Lundell TK, Saranpää P, Kilpäinen I, Teeri TH, Fagerstedt KV (2004) The dibenzodioxocin lignin substructure is abundant in the inner part of the secondary wall in Norway spruce and silver birch xylem. Planta 218:497–500
37. Kukkola E, Saranpää P, Fagerstedt K (2008) Juvenile and compressed wood cell walls layers differ in lignin structure in Norway spruce and Scots pine. IAWA J 29:47–54
38. Donaldson L (2007) Cellulose microfibril aggregates and their size variation with cell wall type. Wood Sci Technol 41:443–460